crystals

MDPI

Article

Trapping Capability of Small Vacancy Clusters in the α-Zr Doped with Alloying Elements: A First-Principles Study

Rongjian Pan [1,*], Aitao Tang [2], Jiantao Qin [1], Tianyuan Xin [1], Xiaoyong Wu [1,3], Bang Wen [1,3] and Lu Wu [1,3]

1 The First Sub-Institute, Nuclear Power Institute of China, Chengdu 610005, China; qjtuestc@163.com (J.Q.); xintianyuan0827@126.com (T.X.); wuxynpic@126.com (X.W.); wilburbwen@126.com (B.W.); wulu1002@126.com (L.W.)
2 College of Materials Science and Engineering, Chongqing University, Chongqing 400044, China; tat@cqu.edu.cn
3 National Key Laboratory for Nuclear Fuel and Materials, Nuclear Power Institute of China, Chengdu 610041, China
* Correspondence: haoyunjiuzhe2008@126.com

Abstract: Zirconium alloys are subjected to a fast neutron flux in nuclear reactors, inducing the creation of a large number of point defects, both vacancy and self-interstitial. These point defects then diffuse and can be trapped by their different sinks or can cluster to form larger defects, such as vacancy and interstitial clusters. In this work, the trapping capability of small-vacancy clusters (two/three vacancies, V_2/V_3) in the α-Zr doped with alloying elements (Sn, Fe, Cr, and Nb) has been investigated by first-principle calculations. Calculation results show that for the supercells of α-Zr containing 142-zirconium atoms with the two-vacancy cluster, alloying elements of Sn and Nb in the second vacant site (V2) and Cr in the first vacant site (V1) are more easily trapped by two vacancies, respectively. However, the two sites are both captured more easily by two vacancies for Fe in the supercells of α-Zr containing 142-zirconium atoms inside due to the similar value of the Fermi level. For the supercells of α-Zr containing 141-zirconium atoms with the three-vacancy cluster, the alloying element of Sn in the third vacant site (V′3), Fe in the first vacant site (V′1), and Cr and Nb in the second vacant site (V′2) are more easily trapped by three vacancies, respectively.

Keywords: zirconium alloys; first-principle calculations; DFT; defect clusters; electronic properties

check for updates

Citation: Pan, R.; Tang, A.; Qin, J.; Xin, T.; Wu, X.; Wen, B.; Wu, L. Trapping Capability of Small Vacancy Clusters in the α-Zr Doped with Alloying Elements: A First-Principles Study. *Crystals* **2022**, *12*, 997. https://doi.org/10.3390/cryst12070997

Academic Editors: Sergio Brutti and David Holec

Received: 1 June 2022
Accepted: 12 July 2022
Published: 18 July 2022

Publisher's Note: MDPI stays neutral with regard to jurisdictional claims in published maps and institutional affiliations.

Copyright: © 2022 by the authors. Licensee MDPI, Basel, Switzerland. This article is an open access article distributed under the terms and conditions of the Creative Commons Attribution (CC BY) license (https://creativecommons.org/licenses/by/4.0/).

1. Introduction

Zirconium alloys are widely used in nuclear power reactors in view of their special properties such as good corrosion resistance, adequate mechanical properties, and a low capture cross section for thermal neutrons [1–3]. A large number of point defects in zirconium alloys under a fast neutron flux are created, such as vacancies and self-interstitials. These point defects can then evolve to small defect clusters, which significantly influence the in-pile performance of zirconium alloys [4–6]. Alternatively, the stability of small-vacancy clusters in zirconium has been investigated using first-principle calculations [7]. The addition of alloying elements is useful to modify the comprehensive mechanical properties of zirconium alloys. However, the understanding of the alloying elements' effect on the small defect clusters in the zirconium alloys induced by neutron irradiation is still insufficient. The stacking fault energies (SFEs) can be predicted by using first-principle calculations based on density functional theory (DFT), which may increase the understanding of responsibility for doped solutes for the deformation modes [8–11]. Therefore, first-principle calculations are capable of predicting the structure stability. Previous works show the structural and electronic properties of one-vacancy and vacancy clusters in the α-Zr [12]. However, the trap capability of small-vacancy clusters doped with alloying elements (Sn, Fe, Cr, and Nb) in the α-Zr has rarely been reported, especially for theoretical investigations.

In order to deeply recognize the effect of doped alloying elements on the trapping capability of small-vacancy clusters in zirconium, it is essential to understand the preliminary formation and evolution of vacancy-alloying element complexes in the zirconium alloys under irradiation conditions. First-principle calculations can provide reliable structural and thermodynamic properties of defects in materials, therefore, in the present work, the trapping capability of small-vacancy clusters (two/three vacancies) in the α-Zr doped with alloying elements are considered here by calculating these electronic properties using first-principle calculations based on DFT.

2. Methodology

The calculations were performed using the Vienna Ab initio Simulation Package (VASP) [13]. The interaction between ions and valence electrons is described by Projector-Augmented Wave (PAW) [14,15]. The generalized gradient approximation (GGA) in the Perdew–Burke–Ernzerhof (PBE) form is used to handle the electron exchange correlations [16]. The plane–wave cut-off energy was set as 400 eV. The first order Methfessel–Paxton with smearing of 0.2 eV was used for the structural relaxation until the total energy changes were within 10^{-6} eV. Meanwhile, the spin polarization of dope atom herein was not taken into consideration during geometric optimization. The structural optimization was performed by relaxing the atomic positions as well as the shape and volume of the supercell. Then, the total energy was calculated using the linear tetrahedron method with Blöchl correction [17]. The Brillouin zone was sampled using a Monkhorst–Pack mesh of *k*-points [18] as follows: $4 \times 5 \times 1$ for $Zr_{142}-V_1$–X_1 and $Zr_{141}-V_2$–X_1 supercells, where V_n stands for the number of vacancies, X_1 is a type of alloying element considered here, such as Sn, Fe, Cr, or Nb. The electron configurations of each of the elements are as follows: Zr ($4d^2 5s^2$), Sn ($5s^2 5p^2$), Fe ($3d^6 4s^2$), Cr ($3d^5 4s^1$), and Nb ($4d^4 5s^1$).

3. Result and Discussion

In order to investigate the trap capability of small-vacancy clusters (two/three vacancies) in the α-Zr doped with alloying elements considered here, two cases are listed. One is a 142-atom supercell with two different vacant lattice sites for one vacancy and one alloying element and the other is a 141-atom supercell with three different vacant lattice sites for two vacancies and one alloying element, as shown in Figure 1.

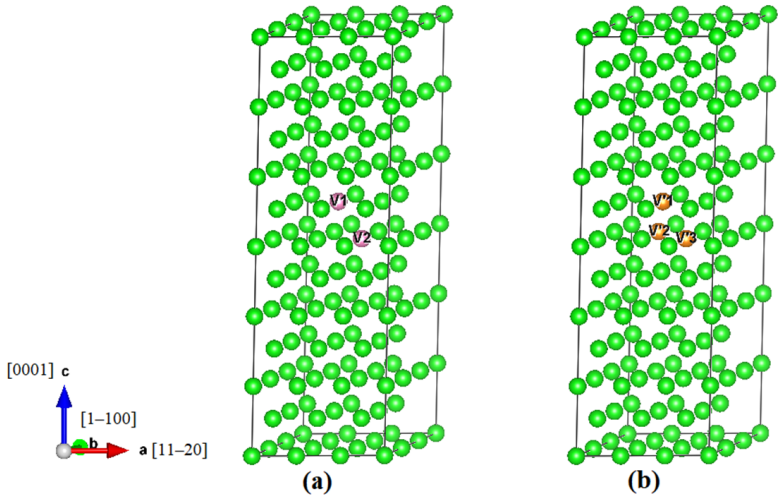

Figure 1. Supercells of pure α-Zr containing (**a**) 142-atom supercell with two different vacant lattice sites for one vacancy and one alloying element, (**b**) 141-atom supercell with three different vacant lattice sites for two vacancies and one alloying element.

3.1. The Formation Energy for V_n and Trapping Energy for V_n–X

According to the ref. [19], the formation energy for V_n is given by:

$$E^f_{V_n} = E_{defect} - \left[E_{without\ defect} - nE(\mathrm{Zr})\right] \quad (1)$$

where E_{defect} and $E_{without\ defect}$ are the energy of the system with and without the defect, respectively. $E(\mathrm{Zr})$ is the energy per atom of the Zr; these Zr atoms removed to build vacancy clusters. n is the number of vacancies; here n = 2 or 3.

Based on Formula (1), it can result that the formation energies for V_2 in pure α-Zr supercell of 144 atomic sites with 142 zirconium atoms (E^f_2) and V_3 in pure α-Zr supercell of 144 atomic sites with 141 zirconium atoms (E^f_3) are 3.90 and 6.23 eV, respectively. It can result that the value of E^f_3 is larger than E^f_2 because the number of bonds between Zr atoms decrease or the surface (vacancy) area increases. It may confer that V_2 is easier to produce than V_3 during irradiation.

According to the ref. [20], the trapping energy of V_n–X is defined as:

$$E^{trap}_{V_n-\mathrm{X}} = E_{V_{n-1}-\mathrm{X}} - E_{V_n} - E_{N\mathrm{Zr},\mathrm{X}} + E_{V_1} \quad (2)$$

where $E_{V_{n-1}-\mathrm{X}}$, E_{V_n}, and E_{V_1} are the total energies of V_{n-1}–X, V_n, and V_1, respectively. N is the total number of Zr atoms for perfect one, n is the number of vacancies; here n = 2 or 3. $E_{N\mathrm{Zr},\mathrm{X}}$ is the energy of the Zr supercell with alloying element X.

The V1 and V′2 sites are considered for the calculation of trapping energies of V_n–X(n = 2, 3) due to both the V1 and V2 sites in the V_2, V′2 and V′3 sites in V_3 being equivalent, respectively. Based on Formula (2), the trapping energies for V_n–X (n = 2, 3), as listed in Table 1. Table 1 illustrates the trapping energies for V_n–X (n = 2, 3); one can see that the order of trapping energies for the alloying element considered here is Fe > Sn > Cr > Nb. The more negative the value of trapping energy the easier the solute atom can be trapped in the small-vacancy clusters. It indicates thus that the sequence of the tapping capability of two-vacancy clusters for the alloying elements considered here is Nb > Cr > Sn > Fe, which is the same situation as the three-vacancy clusters. Alternatively, the influence of the difference in atomic radius between alloying element herein and Zr atom on the trapping energy has been discussed [21]. The larger the mismatch in atomic radius of the target atom in host Zr atom, the lower the trapping energy of V_n–X values, except for Sn. Based on the results of the formation energy for V_n and the trapping energy for V_n–X, one may confer that the vacancy mobility may be lower in the presence of Nb compared with the other three elements considered here; this may be related to the binding energies of small-vacancy clusters with these elements. Thus, it would be useful to know the effect of different dopants on vacancy diffusion.

Table 1. The trapping energies for V_n–X (in eV); here n = 2 or 3.

V_n–X	Trapping Energies
V_2–Sn (Sn in the V1 or V2 site)	−0.26
V_2–Fe (Fe in the V1 or V2 site)	−0.22
V_2–Cr (Cr in the V1 or V2 site)	−0.31
V_2–Nb (Nb in the V1 or V2 site)	−0.37
V_3–Sn (Sn in the V′1 site)	−0.40
V_3–Fe (Fe in the V′1 site)	−0.34
V_3–Cr (Cr in the V′1 site)	−0.45
V_3–Nb (Nb in the V′1 site)	−0.56
V_3–Sn (Sn in the V′2 or V′3 site)	−0.44
V_3–Fe (Fe in the V′2 or V′3 site)	−0.39
V_3–Cr (Cr in the V′2 or V′3 site)	−0.48
V_3–Nb (Nb in the V′2 site or V′3 site)	−0.63

3.2. Atomic Structures and Charge Density Distribution

Figure 2 shows two atomic structures of supercells of α-Zr containing (a) a 142-atom supercell with two different vacant lattice sites for one vacancy and one alloying element, (b) a 141-atom supercell with three different vacant lattice sites for two vacancies and one alloying element, respectively, where the differences of charge density caused by the solute and vacancy are also visualized.

Comparing four different atomic structures of the 142-atom supercell with two different vacant lattice sites for one vacancy and one alloying element, as shown in Figure 2a, one can find that all the atoms have kept their lattice sites for the 142-atom supercell with two different vacant lattice sites, as shown in Figure 2a to Figure 2d, respectively. The value of the isosurface for each charge density distribution figure is 0.035 e/bohr^3. Thus, based on the analysis of atomic structures and the charge density distribution for these supercells, it seems the supercell of 142-Zr atoms with two different vacant lattice sites for one vacancy and one alloying element are stable structures, as shown in Figure 2a to Figure 2d, respectively. In terms of the supercell of 141-Zr atoms with three different vacant lattice sites for two vacancies and one alloying element, it has a similar result to the supercell of 142-Zr atoms with two different vacant lattice sites for one vacancy and one alloying element, as shown in Figure 2e to Figure 2h, respectively. Furthermore, in order to discern which atomic structure considered here is most stable for the supercell of 142-Zr atoms with two different vacant sites for one vacancy and one alloying element and the supercell of 141-Zr atoms with three different vacant lattice sites for two vacancies and one alloying element, it should be made out by the total state density of these atomic structures, as seen in Section 3.3.

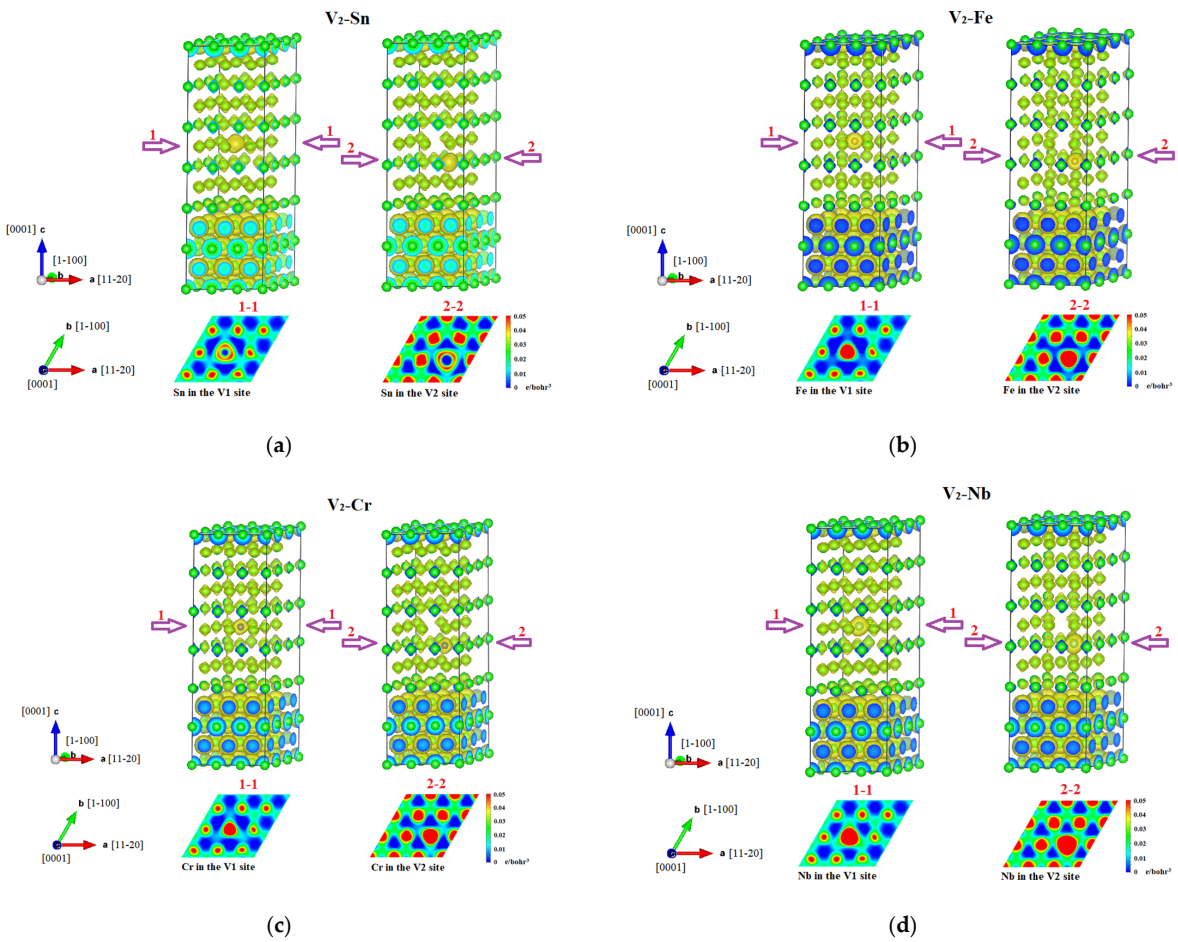

Figure 2. *Cont.*

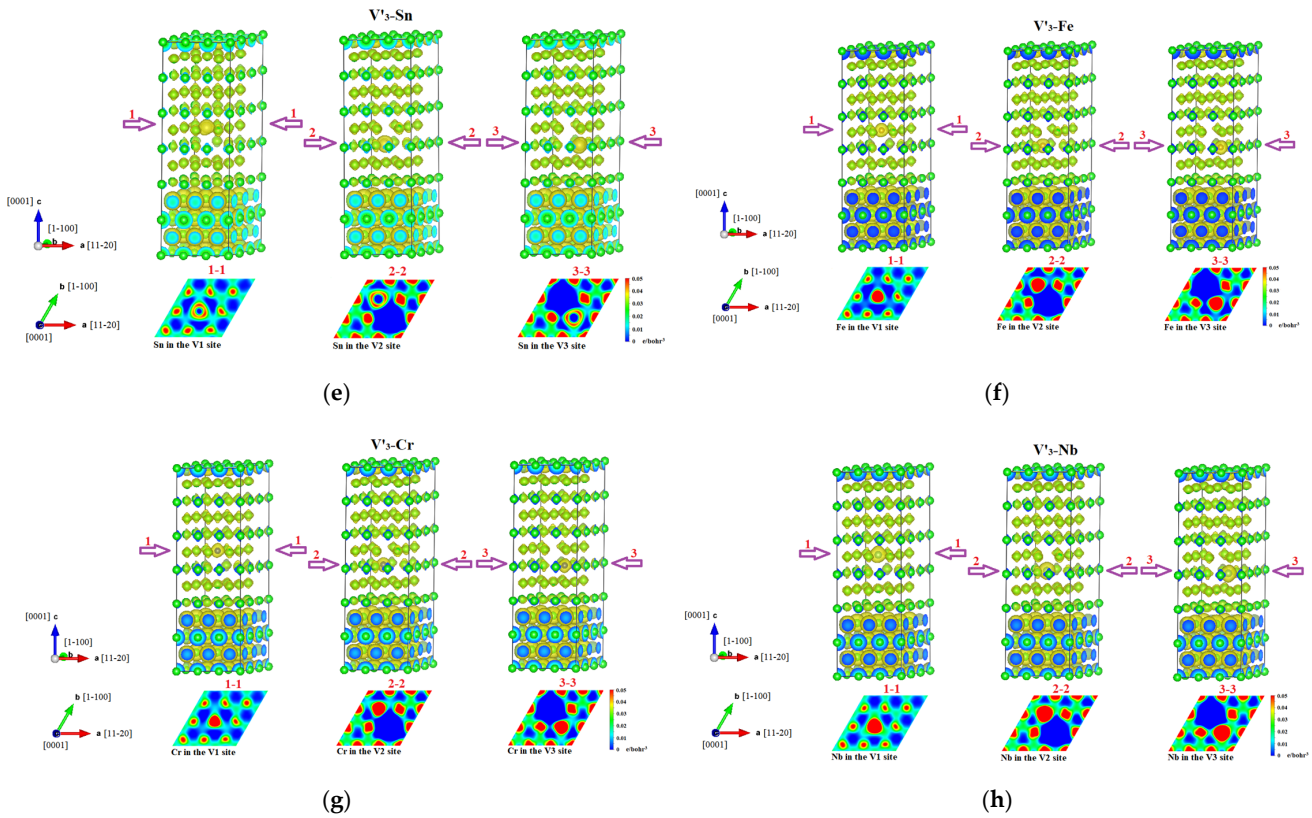

Figure 2. (**a**−**d**) Atomic structure and charge density distribution of 142-atom supercells, and (**e**−**h**) 141-atom supercells with different sites for one vacancy, two vacancy, and one alloying element Sn, Fe, Cr, or Nb. The figures were rendered with VESTA code [22].

3.3. Total Electronic Densities of States (TDOS)

Figure 3 shows a series of total electronic densities of states (TDOS) of a 142-atom supercell with two different vacant lattice sites for one vacancy and one alloying element and a 141-atom supercell with three different vacant lattice sites for two vacancies and one alloying element as indicated before. Besides the supercell with different lattice sites and vacancies, the character of the metallic band is always preserved. The TDOS levels in the [−0.5, 0] eV below the Fermi level are slightly lowered, which implies a lowering of the metallic cohesive strength for these Zr atoms. It means the less the value of the Fermi level, the more stable the structure is. According to this rule, it can achieve the following results. In one case of supercells of pure Zr containing 142-Zr atoms with one vacancy for solute atoms such as alloying elements of Sn and Nb, solute elements of Sn and Nb in the second site (V2) are more easily trapped by two vacancies. In one case of alloying element Cr, solute atom Cr doped in the first site (V1) is more easily trapped by two vacancies. However, two sites for solute atom Fe in supercells of α-Zr containing 142-Zr atoms are more easily trapped by two vacancies due to the similar value of the Fermi levels. In another case of supercells of α-Zr containing 141-Zr atoms with three vacancies, alloying element of Sn in the third site (V3), solute atom Fe in the first site (V1), and solute atoms Cr and Nb in the second site (V2) are more easily trapped by three vacancies, respectively.

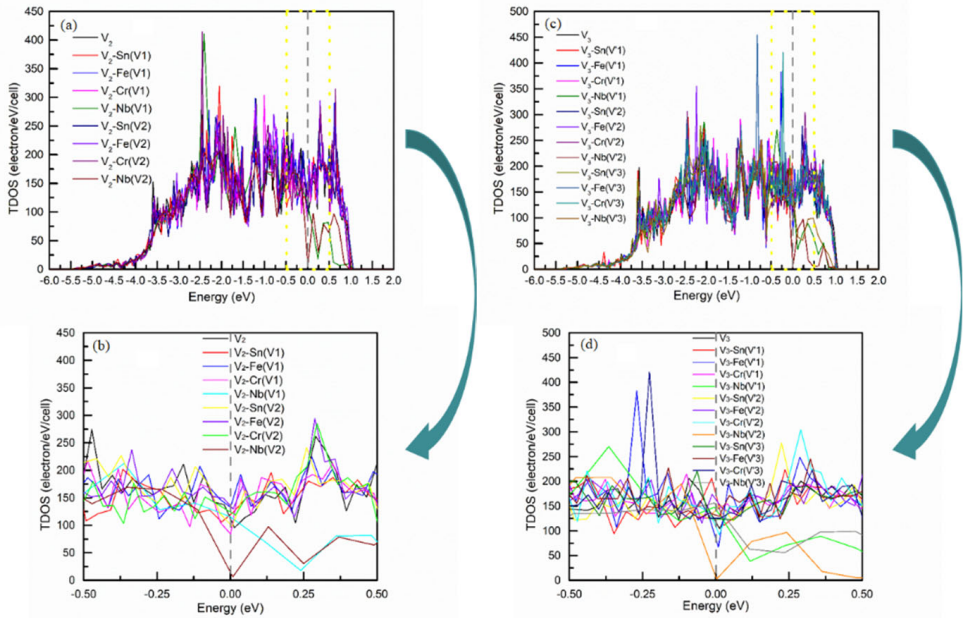

Figure 3. TDOSs of a different number of zirconium atom supercells with different sites for one vacancy (**a**,**b**), or two vacancies (**c**,**d**), and one alloying element (Sn, Fe, Cr, or Nb); where the silver line stands for the Fermi level.

4. Conclusions

The trapping capability of small-vacancy clusters in the α-Zr doped with alloying elements considered here are investigated using first-principle calculations. Based on the atomic structures, charge density distribution, and total electronic densities of states (TDOS) of supercells of pure α-Zr containing bi-vacancies and tri-vacancies doped with one alloying element considered here, it is found that alloying elements of Sn and Nb in the second site and Cr in the first site are more easily trapped by two vacancies in the supercells of α-Zr containing 142-Zr atoms, respectively. However, two sites for Fe are more easily trapped by three vacancies in supercells of α-Zr containing 142-Zr atoms due to the similar value of the Fermi levels. The alloying element of Sn in the third site, Fe in the first site, and Cr and Nb in the second site are more easily trapped by three vacancies in the supercells of α-Zr containing 141-Zr atoms, respectively. Thus, based on the calculation results above, it may help to explore the kinetic evolution and formation mechanism of the microstructure of vacancy-alloying element complexes under irradiation and the associated macroscopic behavior.

Author Contributions: Conceptualization, R.P.; Data curation, J.Q. and R.P.; Formal analysis, T.X. and R.P.; Funding acquisition, R.P.; Investigation, J.Q. and R.P.; Methodology, R.P. and A.T.; Project administration, R.P.; Resources, A.T., X.W., B.W. and L.W.; Software, A.T.; Supervision, R.P.; Validation, R.P. and A.T.; Visualization, A.T.; Writing—original draft, R.P.; Writing—review and editing, R.P., A.T., X.W., B.W. and L.W. All authors have read and agreed to the published version of the manuscript.

Funding: This work is supported by the International Science and Technology Cooperation Project of Sichuan Province, China (No. 2022YFH0043), and the Leading and Innovation Program of China National Nuclear Corporation (No. JJXM–JTLC–2020–02).

Institutional Review Board Statement: Not applicable.

Informed Consent Statement: Not applicable.

Data Availability Statement: Not applicable.

Acknowledgments: This work is supported by the Leading and Innovation Program of China National Nuclear Corporation (No. JJXM-JTLC-2020-02), and the International Science and Technology Cooperation Project of Sichuan Province, China (No. 2022YFH0043).

Conflicts of Interest: The authors declared that they have no conflict of interest in this work. We declare that we do not have any commercial or associative interest that represents a conflict of interest in connection with the work submitted.

References

1. Njifon, I.C.; Torres, E. A first principles investigation of the hydrogen-strain synergy on the formation and phase transition of hydrides in zirconium. *Acta Mater.* **2021**, *202*, 222–231. [CrossRef]
2. Sklenicka, V.; Kral, P.; Kucharova, K.; Kvapilova, M.; Dvorak, J.; Kloc, L. Thermal creep fracture of a Zr1%Nb cladding alloy in the α and (α+β) phase regions. *J. Nucl. Mater.* **2021**, *553*, 152950. [CrossRef]
3. Liu, J.; He, G.; Callow, A.; Li, K.; Moore, K.L.; Nordin, H.; Moody, M.; Lozano-Perez, S.; Grovenor, C.R.; Cuddihy, M.A.; et al. The role of β-Zr in a Zr-2.5Nb alloy during aqueous corrosion: A multi-technique study. *Acta Mater.* **2021**, *215*, 117042. [CrossRef]
4. Hatami, F.; Feghhi, S.A.H.; Arjhangmehr, A.; Esfandiarpour, A. Interaction of primary cascades with different atomic grain boundaries in α-Zr: An atomic scale study. *J. Nucl. Mater.* **2016**, *480*, 362–373. [CrossRef]
5. Arjhangmehr, A.; Feghhi, S.A.H. Irradiation deformation near different atomic grain boundaries in α-Zr: An investigation of thermodynamics and kinetics of point defects. *Sci. Rep.* **2016**, *6*, 23333. [CrossRef] [PubMed]
6. Zhou, W.; Tian, J.; Zheng, J.; Xue, J.; Peng, S. Dislocation-enhanced experimental-scale vacancy loop formation in hcp Zirconium in one single collision cascade. *Sci. Rep.* **2016**, *6*, 21034. [CrossRef]
7. Varvenne, C.; Mackain, O.; Clouet, E. Vacancy clustering in zirconium: An atomic-scale study. *Acta Mater.* **2014**, *78*, 65–77. [CrossRef]
8. Salman, S.; Rekik, N.; Abuzir, A.; Alshoaibi, A.; Suleiman, J. The effect of an external electric field on the electronic properties of defective CBN nanotubes: A density functional theory approach. *Crystals* **2022**, *12*, 321. [CrossRef]
9. Pan, R.; Tang, A.; Wang, Y.; Wu, X.; Wu, L. Effect of alloying elements (Sn, Fe, Cr, Nb) on mechanical properties of zirconium: Generalized stacking-fault energies from first-principles calculations. *Comput. Condens. Matter* **2017**, *10*, 22–24. [CrossRef]
10. Pan, R.; Tang, A.; Wu, X.; Wu, L.; He, W. Effect of the evolution of electronic properties on twin-boundary segregation energies of zirconium form first-principles calculations. *Mater. Lett.* **2017**, *204*, 112–114. [CrossRef]
11. Pan, R.; Tang, A.; Wu, X.; Wu, L.; He, W.; Wen, B.; Zheng, T.; Wang, H. Effect of nonmetallic solutes on the stability of {10–12} tension twin boundary of zirconium: A first-principles study. *Eur. Phys. J. B* **2019**, *92*, 127. [CrossRef]
12. Kharchenko, V.O.; Wu, X.; Wen, B.; Wu, L.; Zhang, W. An atomic sacle study of structural and electronic properties for α-zirconium with single vacancies and vacancy clusters. *Metallofiz. Noveishie Tekhnol.* **2016**, *38*, 1195–1212. [CrossRef]
13. Kresse, G.; Furthmüller, J. Efficient iterative schemes for ab initio total-energy calculations using a plane-wave basis set. *Phys. Rev. B* **1996**, *54*, 11169–11186. [CrossRef] [PubMed]
14. Hohenberg, P.; Kohn, W. Inhomogeneous Electron Gas. *Phys. Rev.* **1964**, *136*, B864–B871. [CrossRef]
15. Kohn, W.; Sham, L.J. Self-Consistent Equations Including Exchange and Correlation Effects. *Phys. Rev.* **1965**, *140*, A1133–A1138. [CrossRef]
16. Perdew, J.P.; Burke, K.; Ernzerhof, M. Generalized gradient approximation made simple. *Phys. Rev. Lett.* **1996**, *7*, 3865–3868. [CrossRef]
17. Blöchl, P.E.; Jepsen, O.; Andersen, O.K. Improved tetrahedron method for Brillouin-zone integrations. *Phys. Rev. B* **1994**, *49*, 16223–16233. [CrossRef]
18. Monkhorst, H.J.; Pack, J.D. Special points for Brillouin-zone integrations. *Phys. Rev. B* **1976**, *13*, 5188. [CrossRef]
19. Sampedro, J.M.; del Rio, E.; Caturla, M.J.; Caro, A.; Caro, M.; Perlado, J.M. Stability of vacancy clusters in FeCr alloys: A study of the Cr concentration dependence. *Nucl. Instrum. Methods B* **2013**, *303*, 46–50. [CrossRef]
20. Zhou, H.B.; Ou, X.; Zhang, Y.; Shu, X.L.; Liu, Y.L.; Lu, G.H. Effect of carbon on helium trapping in tungsten: A first-principles investigation. *J. Nucl. Mater.* **2013**, *440*, 338–343. [CrossRef]
21. Dean, J.A. (Ed.) *Lange's Handbook of Chemistry*, 16th ed.; McGraw-Hill: New York, NY, USA, 2005.
22. Patton, D.C.; Porezag, D.V.; Pederson, M.R. Simplified generalized-gradient approximation and anharmonicity: Benchmark calculations on molecules. *Phys. Rev. B* **1997**, *55*, 7454–7459. [CrossRef]